LOCKHEED MARTIN ENERGY RESEARCH LIBRARIES

3 4456 0515396 3

CENTRAL RESEARCH LIBRARY
DOCUMENT COLLECTION

ORNL-4780

cy. 2

Neutron Elastic- and Inelastic-Scattering Cross Sections for Oxygen in the Energy Range 4.34 to 8.56 MeV

W. E. Kinney

F. G. Perey

OAK RIDGE NATIONAL LABORATORY
CENTRAL RESEARCH LIBRARY
DOCUMENT COLLECTION
LIBRARY LOAN COPY
DO NOT TRANSFER TO ANOTHER PERSON
If you wish someone else to see this document, send in name with document and the library will arrange a loan.
UCN-7969
(3 3-67)

OAK RIDGE NATIONAL LABORATORY

OPERATED BY UNION CARBIDE CORPORATION • FOR THE U.S. ATOMIC ENERGY COMMISSION

Printed in the United States of America. Available from
National Technical Information Service
U.S. Department of Commerce
5285 Port Royal Road, Springfield, Virginia 22151
Price: Printed Copy $3.00; Microfiche $0.95

This report was prepared as an account of work sponsored by the United States Government. Neither the United States nor the United States Atomic Energy Commission, nor any of their employees, nor any of their contractors, subcontractors, or their employees, makes any warranty, express or implied, or assumes any legal liability or responsibility for the accuracy, completeness or usefulness of any information, apparatus, product or process disclosed, or represents that its use would not infringe privately owned rights.

ORNL-4780
UC-34 — Physics

Contract No. W-7405-eng-26

Neutron Physics Division

NEUTRON ELASTIC- AND INELASTIC-SCATTERING CROSS SECTIONS FOR OXYGEN IN THE ENERGY RANGE 4.34 to 8.56 MeV

W. E. Kinney and F. G. Perey

APRIL 1972

OAK RIDGE NATIONAL LABORATORY
Oak Ridge, Tennessee 37830
operated by
UNION CARBIDE CORPORATION
for the
U.S. ATOMIC ENERGY COMMISSION

LOCKHEED MARTIN ENERGY RESEARCH LIBRARIES

3 4456 0515396 3

CONTENTS

Page No.

Abstract 1

Introduction 1

Data Acquisition 1

Data Reduction 3

Results 6

Elastic Scattering 7

Inelastic Scattering 12

Conclusions 17

Acknowledgements 18

Appendix 21

NEUTRON ELASTIC- AND INELASTIC-SCATTERING CROSS SECTIONS FOR OXYGEN IN THE ENERGY RANGE 4.34 TO 8.56 MeV

W. E. Kinney and F. G. Perey

ABSTRACT

We present numerical values for neutron elastic- and inelastic-scattering cross sections for oxygen from 4.34 to 8.56 MeV. Our data are in generally good agreement with the results of others and are well described by ENDF/B evaluations.

INTRODUCTION

We present neutron elastic- and inelastic-scattering cross sections for oxygen in roughly 0.5 MeV intervals between 4.34 and 8.56 MeV. To assist in the evaluation of our data, we briefly discuss our data acquisition and reduction techniques.

For the purposes of discussion, we present our data in graphical form where we compare with the results of others and with ENDF/B 1013 and 4134. Tables of our numerical values of the cross section are given in an appendix.

DATA ACQUISITION

The data were obtained with conventional time-of-flight techniques. Pulsed (2MHz), bunched (~1 nsec full width at half maximum, FWHM) deuterons accelerated by the ORNL Van de Graaff interacted with deuterium in a gas cell to produce neutrons by the $D(d,n)^3He$ reaction. The gas cell, whose length was 1 cm and whose pressure was approximately 1.5 atm, gave neutron energy resolutions in the order of 60 keV.

The neutrons were scattered from solid right circular cylindrical samples placed approximately 10 cm from the gas cell when the detector angles were greater than 25°. For smaller detector angles the cell-to-samples distance had to be increased to as much as 30 cm in order to shield the detector from neutrons coming directly from the gas cell.

The scattered neutrons were detected by 12.5-cm-diam NE-213 liquid scintillators optically coupled to XP-1040 photomultipliers. The scintillators were normally 2.5 cm thick. Data were taken with a single detector and later with three detectors simultaneously. Flight paths varied from 4 to 6 m, with the detector angles ranging from 15 to 140°. The gas-cell neutron production was monitored by a time-of-flight system which used a 5-cm-diam by 2.5-cm-thick NE-213 scintillator viewed by a 58-AVP photomultiplier placed about 4 m from the cell at an angle of 55° with the incident deuteron beam.

The flight time of a detected recoil proton event with reference to a beam pulse signal, the pulse height of the recoil proton event, and identification of the detector in the three-detector system were supplied to an on-line PDP-7 computer. The electronic equipment for supplying this information to the computer consisted, for the most part, of standard commercial components. While gamma rays were discriminated against for both the scattered neutron and the monitor detectors, the discrimination was poor below a neutron energy of 700 keV. A digital bias corresponding to this neutron energy was therefore put into the computer so that two time-of-flight spectra were obtained for each scattered-neutron detector, the spectra corresponding to pulse heights above and below the digital bias. Only the spectra above the bias were used.

The detector efficiencies were measured by (n,p) scattering from a thin (6-mm-diam) polyethylene sample and by detecting neutrons coming directly from the gas cell. Both interactions gave results which were in agreement and which yielded efficiency vs energy curves that compared well with calculations.[1]

DATA REDUCTION

We have developed methods of data reduction which have both simplified the process and made it more reliable. Central to the data reduction process is the use of a light pen with the PDP-7 computer scope display programs to extract peak areas from spectra. The light pen makes a comparatively easy job of separating multiplets and estimating errors in the cross section due to extreme but possible peak shapes. The time-of-flight spectra are transformed into a center-of-mass cross section as a function of excitation energy in the target nucleus before peak stripping is done. This transformation removes kinematic effects and allows easy comparison of spectra taken at different angles or different incident neutron energies. The second effect of the transformation is to make all the peak shapes and widths approximately the same. In the time-of-flight spectrum the width of the peaks is a rapidly varying function of neutron energy since the energy dispersion changes as a function of flight time. Finally, there is a communication between the PDP-7 and larger computers via magnetic tape in order to minimize the bookkeeping and card punching and hence the errors which accompany such operations.

The reduction process starts by normalizing a sample-out to a sample-in time-of-flight spectrum by the ratio of their monitor neutron peak areas, subtracting the sample-out spectrum, and transforming the difference spectrum

into a spectrum of cross section (mb/ster/25 keV) vs excitation energy (25 keV/channel). In addition, a spectrum of the variance is computed based on the counting statistics of the initial data.

The transformed spectra are read into the PDP-7 computer from magnetic tape, and the peak stripping is done by means of the light pen. A peak is stripped by drawing a background beneath it and then having the computer calculate the peak area (mb/ster), centroid, and FWHM. The variance spectrum is used to compute a counting statistics variance corresponding to the stripped peak. Peak stripping errors due to uncertainties in the residual background under the peaks or to the tails of imperfectly resolved nearby peaks may be included with the other errors by stripping the peaks several times corresponding to high, low, and best estimates of this background. Although somewhat subjective, the low and high estimates of the cross sections are identified with 95% confidence limits; these together with the best estimate define upper and lower errors due to stripping. Different upper and lower values of the stripping errors are allowed since the upper and lower estimates of the background are rarely symmetric about the best estimate. When a spectrum is completely stripped, the stripping information is written on magnetic tape for additional processing by a larger computer.

Inelastic cross sections are generally sufficiently isotropic so that finite sample corrections can be made at each angle independent of results at other angles. Correction of the elastic cross section, however, must await the reduction of the entire angular distribution before the finite sample effects can be considered. The corrections are performed according to semianalytic recipes whose constants were obtained from fits to Monte Carlo results.[2]

The final error analysis is performed, including uncertainties in the geometrical parameters (scatterer size, gas cell to scatterer distance, flight paths, etc.) and the uncertainties in the finite sample size corrections.

We fit the corrected differential cross sections and integrate the fitted curve to obtain total elastic and inelastic cross sections. We assume that levels higher than the first excited state are isotropic, take a weighted average of the data, and multiply by 4π to obtain the integrated cross section. The computation of the average is an iterative process in that the data points are tested on each round to see whether or not they lie within 3 of their counting-statistical standard deviations of the current average. If a point fails the test, it is ignored on the next round in the computation of a new average.

The ground state and first excited state are fitted by least squares to a Legendre series:

$$\sigma(\mu = \cos\theta) = \sum_{\ell=0}^{L} \frac{2\ell+1}{2} a_\ell P_\ell(\mu),$$

the points being weighted by the inverse of their average total variance. In order to prevent the fit from giving totally unrealistic values outside the angular range of our measurements, we have resorted to the inelegant but workable process of adding three points equally spaced in angle between the largest angle of measurement and 175°. The differential cross sections at the added points were chosen to reproduce the diffraction pattern at large angles, but were assigned 50% errors.

As pointed out by Rose[3] if the weight of each point in a least squares fitting is equal to the inverse of its variance, then the variances of the coefficients are equal to the diagonal elements in the least squares inverse matrix. For the purpose of calculating the errors in the coefficients, the errors of the three added points are reduced to 10%.

In the case of fitting the elastic cross section, we have the option of including Wick's limit as an additional data point with an error calculated from the error in the total cross section combined with the 7% error we attribute to the error in efficiency.

RESULTS

The scattering sample was water contained in a right circular can made of 7-mil stainless steel of mass 2.66 g, diameter 1.61 cm, and height 2.68 cm. The can held approximately 4.5 g of water. Data taken with an empty can were used to subtract the effects of the can. At angles greater than 10° the hydrogen elastic peak was well separated from the oxygen peak and caused no difficulty.

We first present our differential elastic-scattering cross sections in graphical form and compare them with the results of others and with ENDF/B evaluations 1013 (Ref. 4) and 4134 (Ref. 5). Our differential cross sections for inelastic scattering to the (6.052 + 6.131) MeV levels were isotropic within experimental error so no graphs of these differential cross sections are presented. Our integrated elastic and inelastic cross sections as a function of energy are compared with previous results and with the ENDF/B evaluations. The values of the cross sections are tabulated in the appendix.

The abbreviations we use, reference numbers, energies, and energy spreads for the other investigators whose results are compared with ours are given in Table 1.

Elastic Scattering

Our oxygen differential elastic-scattering cross sections are shown in Fig. 1 together with least-squares fits to the data (Wick's limit was not included).

Our results are compared with the results of others and with ENDF/B 1013 in Fig. 2. Our results are consistent with NEL at 7.54 MeV and are in reasonable agreement with PHIL at 6.01 and 7.03 MeV. Our energy spreads are comparable with those of Bostrom et al., but our energies are sufficiently different to account for dis-similarities in the angular distributions in a nucleus as resonant as oxygen. The results of Chase et al. are in fair agreement with ours at 6.01 and 6.44 MeV. Their different energies and larger energy spreads may account for differences in the results. We agree reasonably well with Hill at 4.92 MeV.

ENDF/B 1013 angular distributions above 5 MeV are based upon optical model fits to the data of Chase et al. The forward peaks and first minima are reproduced reasonably well at other energies with the exception of 8.56 MeV.

Oxygen was reevaluated in August 1971 by Young and Foster[5] and released as ENDF/B 4134 (and 1134). Their elastic angular distributions are compared with experimental data in Fig. 3. The distributions are the same as those of ENDF/B 1013 below 5 MeV. Above 5 MeV the data of Phillips[7] was included in the optical model fits, having the effect of raising the distribution at back angles between 5.66 and 7.03 MeV. Otherwise the distributions of 1013 and 4134 are very much the same.

Table 1. Abbreviations, References, Energies, and Energy Spreads for Other Investigators

Abbreviation	Energy, MeV	Reference
NEL	7.55 ± 0.06	6
PHIL	6.0 7.0	7
BOS+	4.30 ± 0.06 4.50 ± 0.06 4.85 ± 0.06 7.11 ± 0.05	8
CHA+	4.99 ± 0.14 5.66 ± 0.145 6.02 ± 0.13 6.53 ± 0.115 8.00 ± 0.32	9
AILL	5.00 ± 0.10	10
K&P	6.72 ± 0.15 6.87 ± 0.15 6.95 ± 0.15 7.02 ± 0.15 7.40 ± 0.12 7.45 ± 0.12 7.50 ± 0.12 7.70 ± 0.12 7.89 ± 0.10 7.93 ± 0.10 8.09 ± 0.10 8.28 ± 0.10 8.55 ± 0.10	11

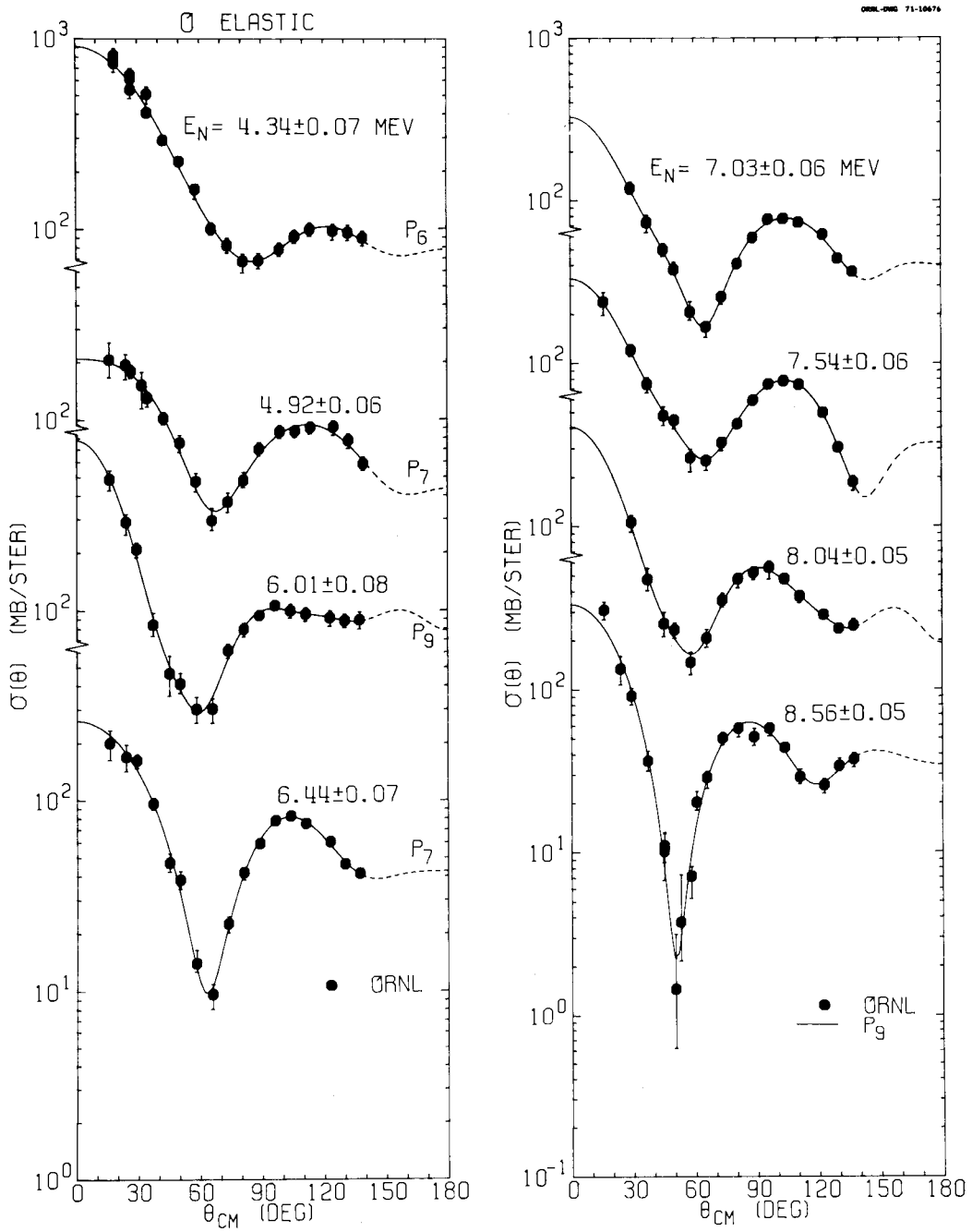

Fig. 1. Our O neutron differential elastic-scattering cross sections with Legendre fits.

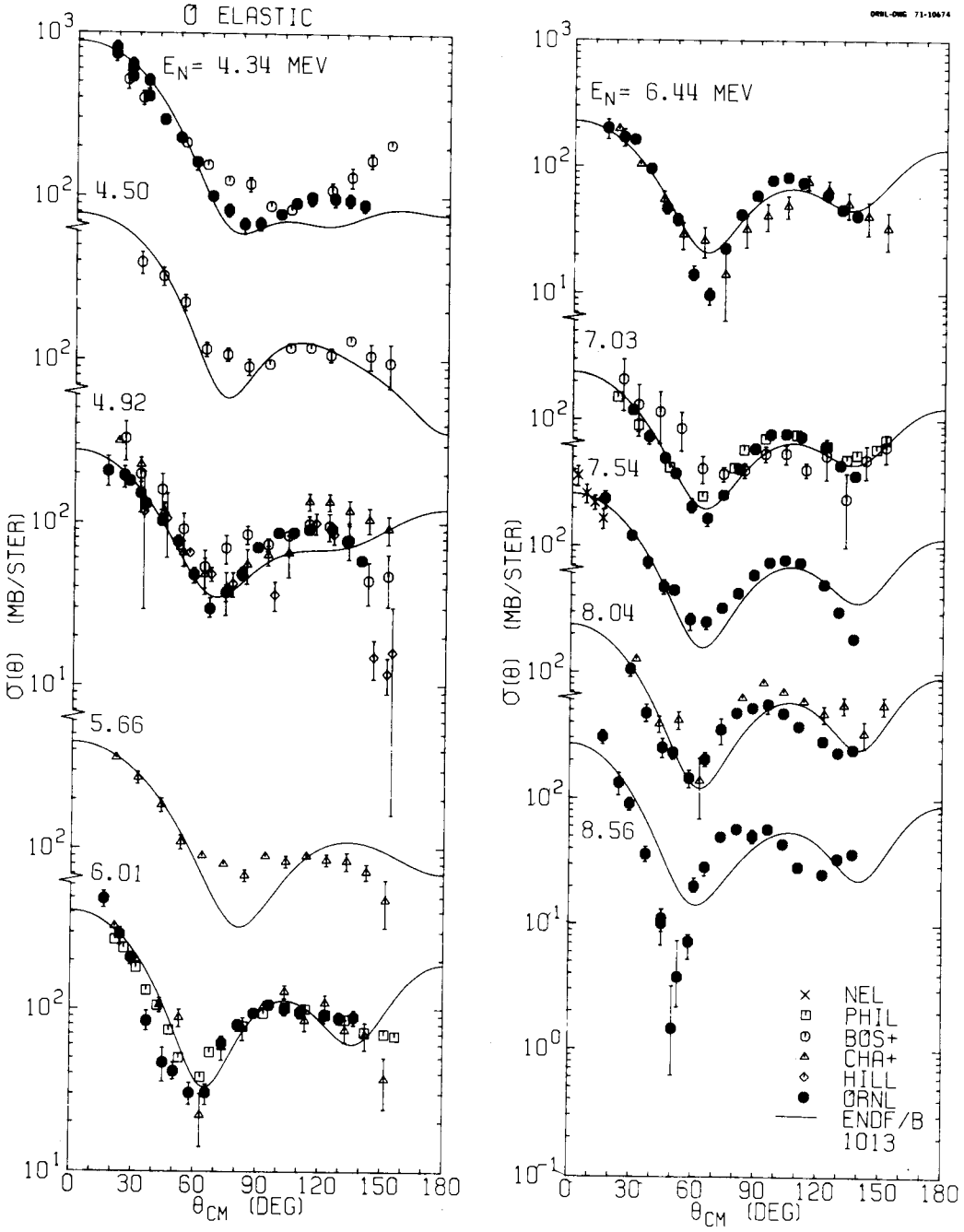

Fig. 2. Experimental O neutron differential elastic-scattering cross sections compared with ENDF/B 1013.

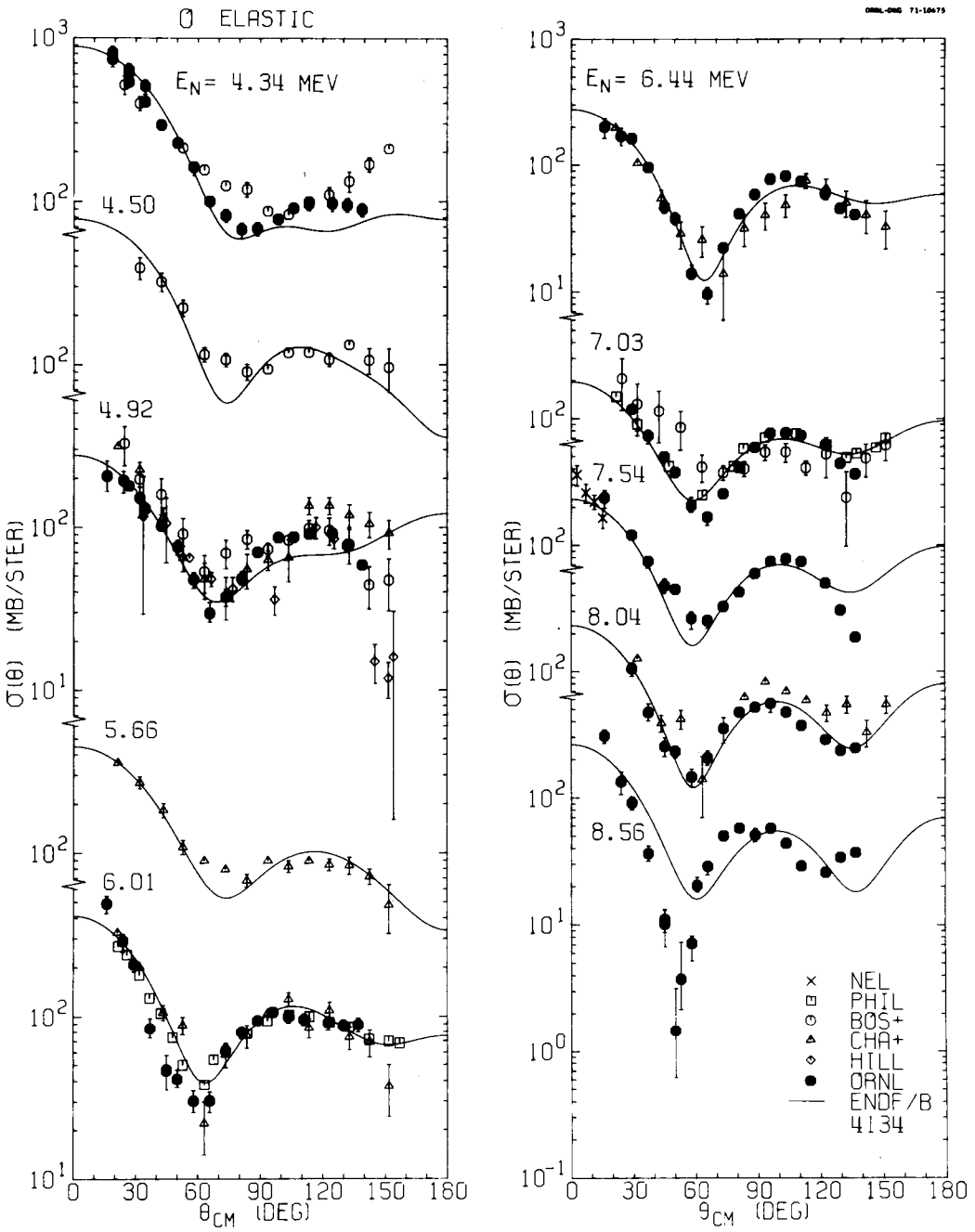

Fig. 3. Experimental O neutron differential elastic-scattering cross sections compared with ENDF/B 4134.

The integrated experimental elastic cross sections as a function of energy are compared in Fig. 4 along with the ENDF/B 1013 values. A comparison is made with ENDF/B 4134 in Fig. 5. One immediately notes the resonant behavior of Oxygen and, where the energies of measurement are sufficiently close, we agree with the results of others for the point of Chase et al. at 8 MeV.

The evaluations are in good agreement with experiments below 7 MeV. The (n,α) reaction is the only reaction competing with elastic scattering below the threshold for inelastic scattering to the 6.052 MeV level since capture is negligible.

Above 7 MeV, neither evaluation agrees with the Chase et al. point at 8 MeV though 4134 is in better agreement than is 1013. Both evaluations agree with our point at 8.04 MeV. Evaluation 1013 is just above our error bar at 7.54 MeV and is about 100 mb higher than our point at 8.56 MeV, whereas 4134 is roughly 200 mb higher at 7.54 MeV and 150 mb higher at 8.56 MeV. These differences in the evaluations are almost entirely due to differences in the cross section for inelastic scattering to the 6.052 + 6.131 MeV levels (see Figs. 6 and 7). Evaluation 1013 excites these levels uniformly more than does 4134 from 6 to 8.5 MeV and at 7.54 and 8.56 MeV by about the differences in their elastic-scattering cross sections.

Inelastic Scattering

Our angle-integrated cross sections for inelastic scattering to the (6.052 + 6.131) levels as a function of energy are compared with ENDF/B 1013 values in Fig. 6 and with ENDF/B 4134 values in Fig. 7. The results of Dickens and Perey[11] for inelastic scattering to the 6.131 MeV level as

ORNL-DWG 72-2758

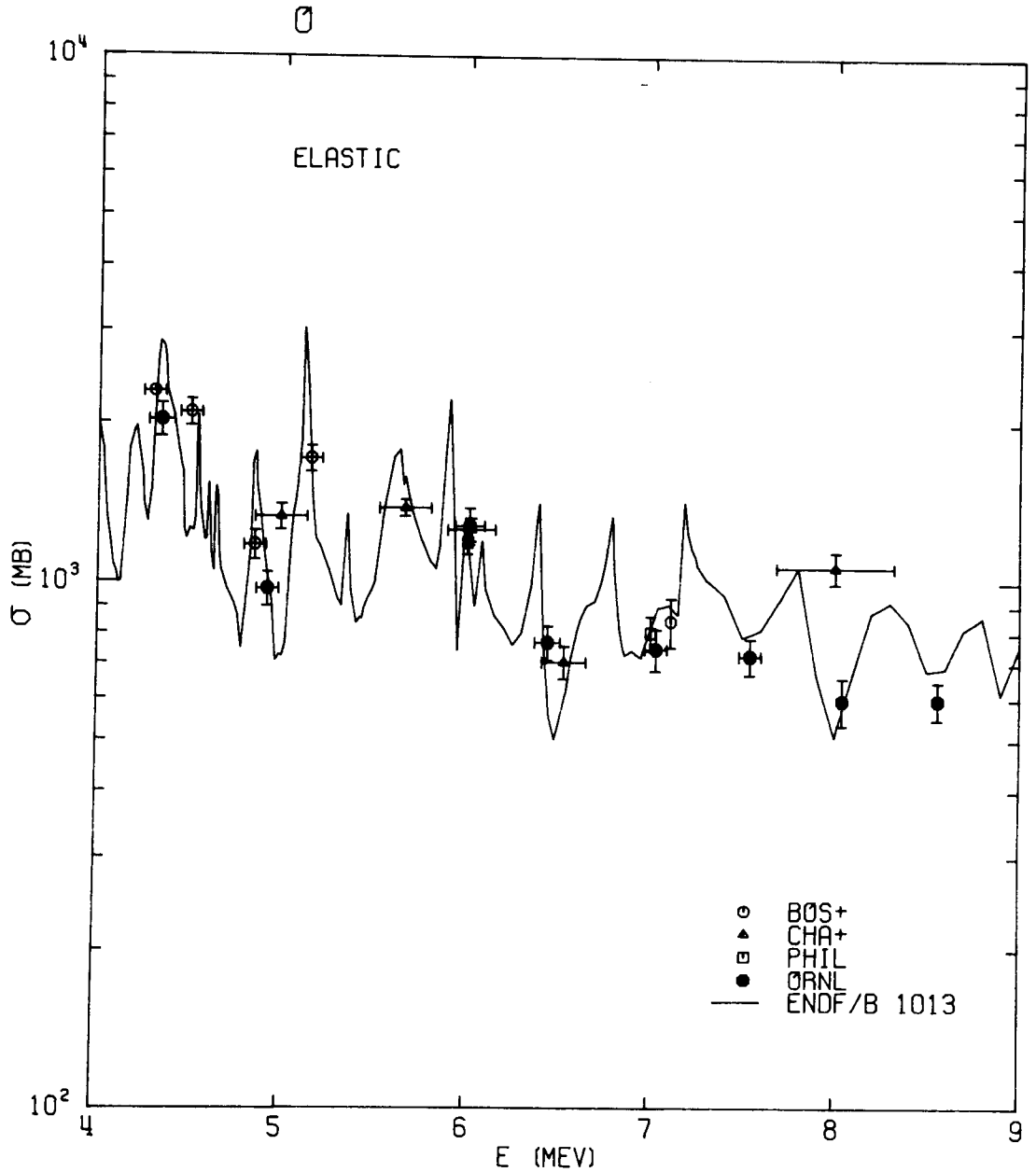

Fig. 4. Experimental integrated elastic-scattering cross sections as a function of energy compared with ENDF/B 1013.

ORNL-DWG 72-2759

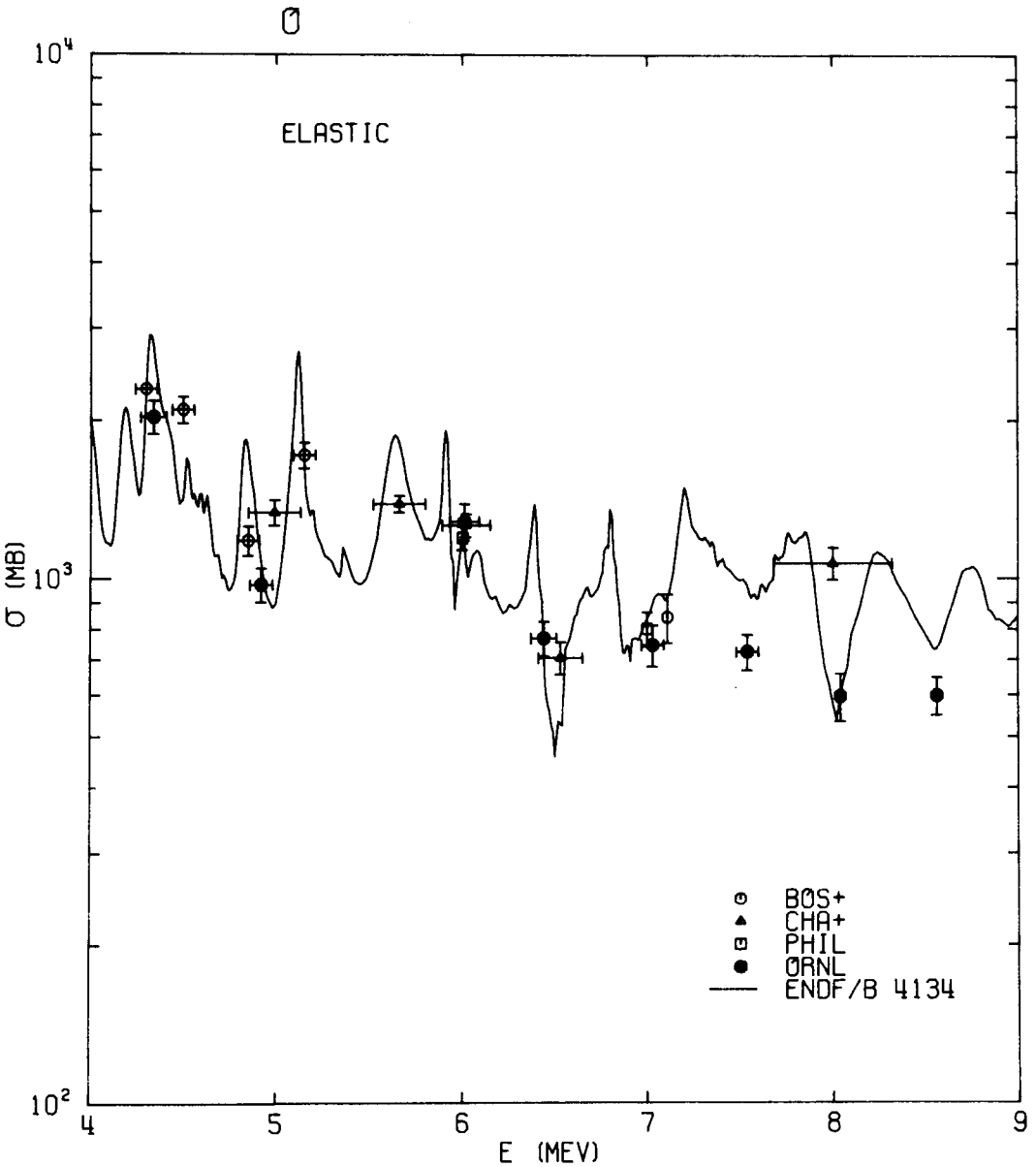

Fig. 5. Experimental integrated elastic-scattering cross sections as a function of energy compared with ENDF/B 4134.

ORNL-DWG 72-2756

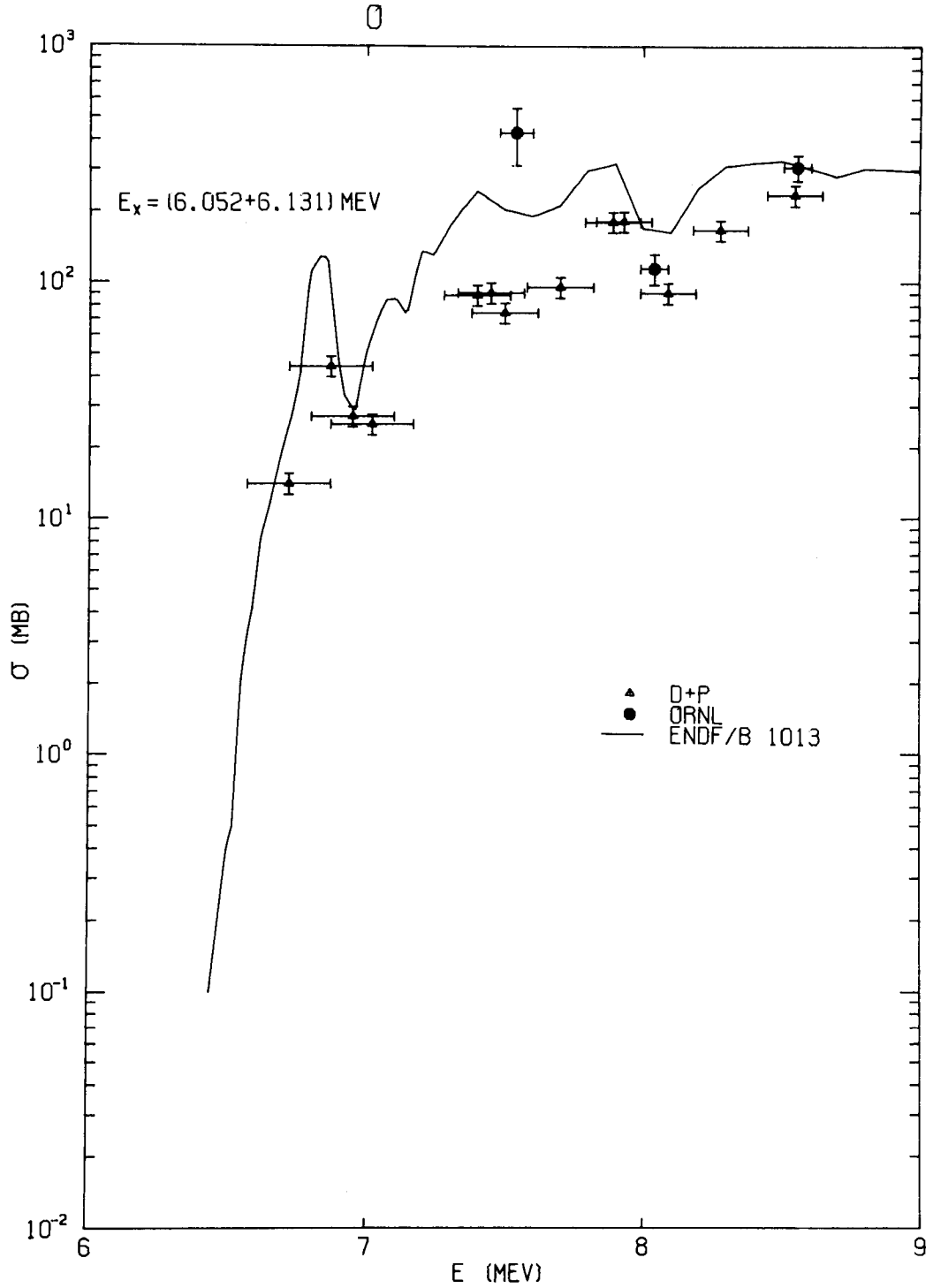

Fig. 6. Experimental integrated cross sections for inelastic scattering to the 6.052 and 6.131 MeV levels in ^{16}O as a function of energy compared with ENDF/B 1013.

ORNL-DWG 72-2757

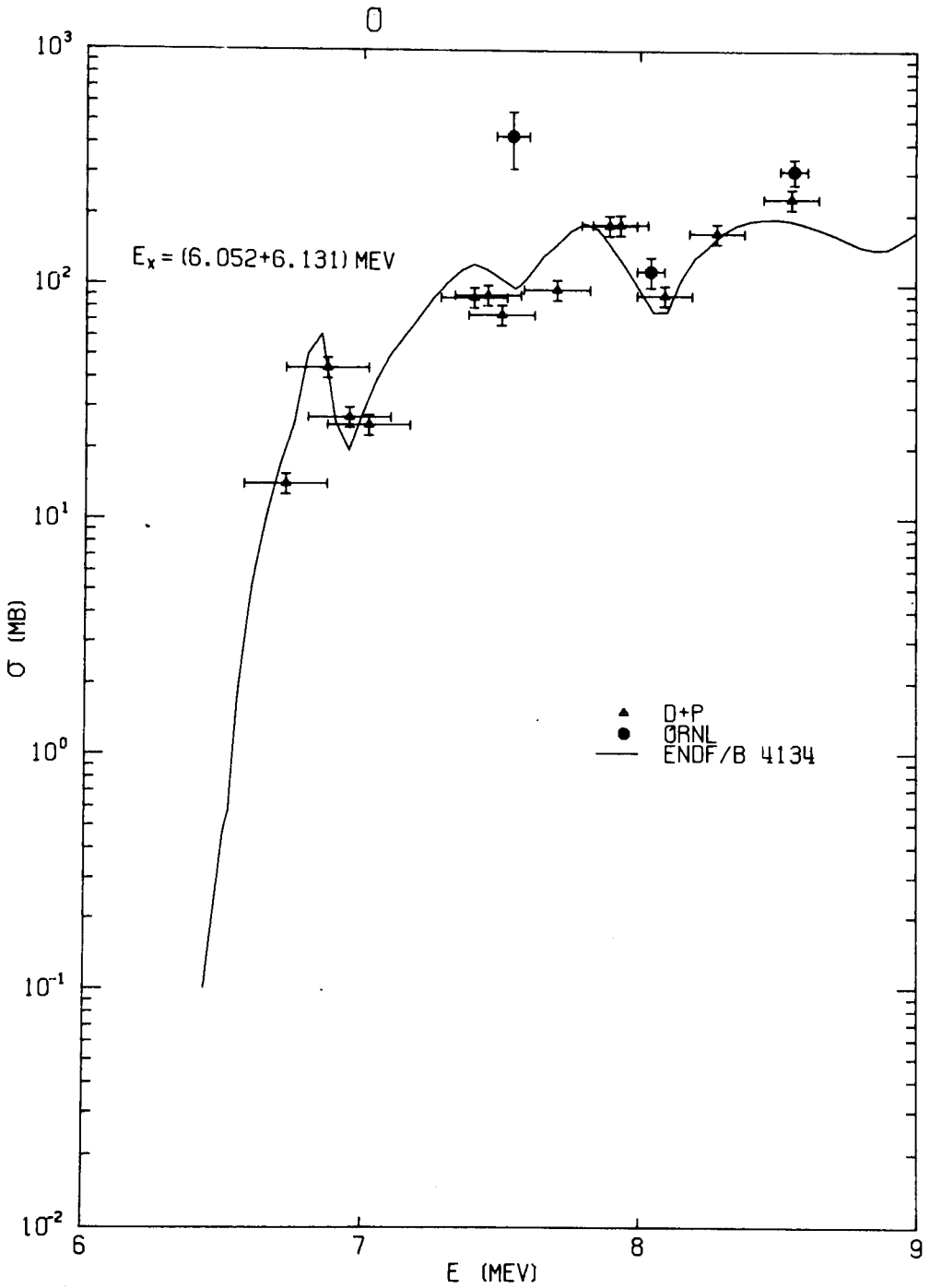

Fig. 7. Experimental integrated cross sections for inelastic scattering to the 6.052 and 6.131 MeV levels in ^{16}O as a function of energy compared with ENDF/B 4134.

determined from 4π times the differential inelastic γ-ray cross section at 55° are also shown in the figures.

Our cross sections should be higher than those of Dickens and Perey since we include inelastic scattering to the 6.052 MeV level. In addition, the 6.131 MeV γ-ray angular distribution may be anisotropic with non-negligible contributions from Legendre polynomials higher than P_2. In fact, the angular distribution of Drake et al.[12] at 7.5 MeV integrates to a value approximately 40% higher than $4\pi \frac{d\sigma}{d\omega}(55^{o})$.

Our results, then, are consistent with those of Dickens and Perey at 8 and 8.5 MeV, but a contribution of ~290 mb due to inelastic scattering to the 6.052 MeV level is necessary to reconcile results around 7.5 MeV. Our electronic bias prevented our measuring the differential cross section at angles greater than 55°. If the angular distribution is peaked forward then our assumption of isotropy in multiplying the average differential cross section by 4π to arrive at the integrated cross section would result in a high value. The value we get, however, is not inconsistent with experimental values of σ_T, σ_S, and $\sigma_{n\alpha}$. Karlsruhe[13] σ_T at 7.54 MeV averaged over our energy spread of ± 0.05 MeV is 1138 ± 33 mb assuming a 3% error. The ENDF/B value for the (n,α) cross section is 60 ± 5 mb. Our integrated elastic scattering cross section is 723 ± 56 mb. These values give $\sigma(n,n') = \sigma_T - \sigma_S - \sigma(n,\alpha) = 355 \pm 65$ for the (n,n') cross section which may be compared with our value of 429 ± 116 mb.

ENDF/B 1013 used the Schmidt tabulation[14] for the (n,n') cross sections below 10 MeV. The cross section for inelastic scattering to the 6.052 MeV level was assumed to be 10% of the cross section for inelastic scattering to the (6.131 + 6.91 + 7.12) MeV levels from 6.5 to 8.5 MeV. ENDF/B 4134

considered the data of Dickens and Perey for excitation of the 6.131 MeV level and used compound nucleus calculations for the 6.052 MeV level.

CONCLUSIONS

The ENDF/B evaluations describe our elastic data well in the important range of angles less than 60° where the distribution peaks forward. It may be questioned whether our data taken ~0.5 MeV apart can be used with confidence to interpolate to other energies in a nucleus so resonant as oxygen.

ACKNOWLEDGEMENTS

Numerous persons have contributed to this experimental program at one time or another and we would like to thank them for their contributions. In particular, we would like to acknowledge the help of J. K. Dickens, J. W. McConnell, J. A. Biggerstaff, A. M. Marusak, P. H. Stelson, C. O. LeRigoleur, and E. Hungerford.

REFERENCES

1. R. E. Textor and V. V. Verbinski, O5S: A Monte Carlo Code for Calculating Pulse Height Distributions Due to Monoenergetic Neutrons Incident on Organic Scintillators, ORNL-4160 (February 1968).

2. W. E. Kinney, Nucl. Instr. and Methods 83, 15 (1970).

3. M. E. Rose, Phys. Rev. 91, 610 (1953).

4. E. L. Slaggie and J. T. Reynolds, ^{16}O Fast Neutron Cross Sections and Legendre Moments Below 15.0 MeV, Knolls Atomic Power Laboratory Report KAPL-M-6452 (April 1965).

5. P. G. Young and D. D. Foster, Jr., Los Alamos Scientific Laboratory Report LA-4780 (to be published).

6. W. P. Bucher, C. E. Hollandsworth, R. D. Lamoreaux, and R. R. Sankey, Nuclear Effects Laboratory, private communication.

7. D. D. Phillips, data given in Angular Distributions in Neutron-Induced Reactions, Volume 1, Z = 1 to 20, BNL-400, Third Edition (January 1970).

8. Norman A. Bostrom, Ira L. Morgan, J. Thomas Prud'Homme, and Abdul R. Sattar, The Elastic Scattering of Fast Neutrons from Oxygen and Nitrogen, WADC Technical Report 57-446 (September 1957).

9. L. F. Chase, Jr., R. G. Johnson, R. V. Smith, F. J. Vaughn, and M. Walt, Fast Neutron Cross Sections of Oxygen and Nitrogen, Lockheed Aircraft Corporation Report AFSWC-TR-61-15 (February 1961).

10. R. W. Hill, Phys. Rev. 109, 2105 (1958).

11. J. K. Dickens and F. G. Perey, Nucl. Sci. Eng. 40, 283 (1970).

12. Darrell M. Drake, John C. Hopkins, C. S. Young, and H. Conde, Nucl. Sci. Eng. 40, 294 (1970).

13. S. Cierjacks, P. Forti, D. Kopsch, L. Kropp, J. Nebe, and H. Unseld High Resolution Total Neutron Cross Sections Between 0.5 - 30 MeV, Kernforschungszentrum Karlsruhe Report KFK 1000 (June 1968).

14. J. J. Schmidt, Neutron Cross Sections for Fast Reactor Materials, Kernforschungszentrum Karlsruhe Report KFK 120 (February 1966).

APPENDIX

Tabulated Values of Neutron Elastic- and Inelastic-Scattering Cross Sections for O in the Energy Range 4.34 to 8.56 MeV

We tabulate below our values of neutron elastic- and inelastic-scattering cross sections for Oxygen. The tables are arranged by level in order of increasing incident neutron energy. The errors in the differential cross sections are relative and do not include a $\pm$ 7% error in efficiency which is common to all points. The uncertainty in angle is $\pm 1^{\circ}$. The integrated cross sections do include the $\pm$ 7% efficiency error.

Table A1. A Table of Contents for the O Neutron Cross Section Tables

Quantity	Page No.
Elastic Scattering	23 - 30
Inelastic Scattering	
E_x = 6.052 + 6.131 MeV	31 - 32

SCATTERING OF 4.34 +OR-0.07 MEV NEUTRONS FROM O

LEVEL(S) 0.0 MEV KEY(11) 20 ANGLES

ANGLE CM	X-SEC. MB/STR	ERROR (O/O) +	ERROR (O/O) -	RUN

MULTIPLE SCATTERING CORRECTION DONE

18.58	742.99	8.4	10.5	28211
18.58	813.51	8.9	9.8	27215
26.52	536.37	5.4	10.1	10211
26.52	640.70	8.8	9.1	28215
26.52	612.56	9.2	11.7	27213
34.43	405.94	6.3	7.2	10215
34.43	508.07	9.0	11.1	28213
42.31	292.08	5.7	7.0	10213
50.15	226.83	6.1	6.7	15911
57.94	161.78	6.2	11.2	15915
65.69	100.38	7.2	7.3	15913
73.38	82.35	8.7	9.1	11811
81.01	67.66	9.1	12.7	11815
88.58	68.36	9.1	9.3	11813
98.58	78.22	8.0	8.0	14311
106.01	91.16	7.7	7.8	14315
113.38	99.37	7.8	8.1	14313
124.57	97.35	8.2	10.4	13211
131.79	95.24	9.5	9.1	13215
138.97	89.34	8.2	9.3	13213

AVERAGE X-SEC 0.0 MB/STR 0 NOTE

INTEGRATED X-SEC 2031.12 MB ERROR 7.3 PER CENT

P 6 FIT

L	COEF.	ERROR (O/O)
0	323.26367	2.1
1	128.79866	4.3
2	91.47656	5.0
3	54.64304	7.1
4	17.45149	18.1
5	5.70827	39.7
6	3.86886	48.6

SCATTERING OF 4.92 +OR-0.06 MEV NEUTRONS FROM O

LEVEL(S) 0.0 MEV KEY(11) 18 ANGLES

ANGLE CM	X-SEC. MB/STR	ERROR(O/O) +	-	RUN
MULTIPLE SCATTERING CORRECTION DONE				
15.93	206.72	23.0	19.3	25211
23.88	194.12	13.8	16.1	25215
26.52	179.96	7.1	7.9	8911
31.80	151.91	16.8	24.3	25213
34.43	130.52	7.1	10.1	8915
42.31	102.02	7.4	7.5	8913
50.15	75.93	9.6	10.6	1511
57.94	47.64	10.2	11.6	1515
65.68	29.64	16.0	11.4	1513
73.38	37.27	11.2	12.3	3411
81.01	48.26	9.8	8.4	3415
88.58	70.34	8.3	7.8	3413
98.58	86.58	7.2	7.8	7611
106.01	87.00	6.5	7.3	7615
113.38	90.84	6.8	7.5	7613
124.56	91.58	7.1	9.7	6011
131.79	77.50	8.0	9.1	6015
138.97	58.54	8.0	7.7	6013

AVERAGE X-SEC 0.0 MB/STR 0 NOTE

INTEGRATED X-SEC 972.18 MB ERROR 7.5 PER CENT

P 7 FIT

L	COEF.	ERROR(O/O)
0	154.72737	2.6
1	18.52838	15.9
2	14.71479	18.4
3	23.47386	9.6
4	4.25453	46.0
5	-3.65671	42.4
6	-1.04994	115.3
7	-0.89900	130.7

SCATTERING OF 6.01 +OR-0.08 MEV NEUTRONS FROM O

LEVEL(S) 0.0 MEV KEY(11) 17 ANGLES

ANGLE CM	X-SEC. MB/STR	ERROR(O/O) +	-	RUN
MULTIPLE SCATTERING CORRECTION DONE				
15.93	488.89	11.3	12.6	51486
23.88	290.17	10.4	14.1	31486
29.16	208.87	8.0	9.5	51456
37.06	84.09	15.8	12.6	31456
44.93	46.55	23.4	23.9	11456
50.15	41.07	13.8	10.7	51465
57.94	30.16	15.8	15.2	31465
65.68	30.27	13.2	15.7	11465
73.37	61.44	8.1	8.7	51449
81.01	79.61	7.7	8.7	31449
88.58	94.11	7.4	5.9	11449
96.09	106.18	6.7	6.7	51472
103.54	99.80	8.0	8.5	31472
110.93	95.72	7.8	8.4	11472
122.63	91.36	8.6	9.9	51479
129.87	87.88	8.5	7.9	31479
137.06	88.89	10.1	10.5	11479

AVERAGE X-SEC 0.0 MB/STR 0 NOTE

INTEGRATED X-SEC 1277.84 MB ERROR 8.0 PER CENT

P 9 FIT

L	COEF.	ERROR(O/O)
0	203.37532	3.8
1	27.61331	21.7
2	39.55038	14.1
3	42.45799	9.8
4	32.42499	11.1
5	16.34143	18.5
6	7.73927	32.1
7	6.34801	36.7
8	3.78395	40.4
9	2.44105	61.5

SCATTERING OF 6.44 +OR-0.07 MEV NEUTRONS FROM O

LEVEL(S) 0.0 MEV KEY(11) 17 ANGLES

ANGLE CM	X-SEC. MB/STR	ERROR (O/O) +	ERROR (O/O) -	RUN
MULTIPLE SCATTERING CORRECTION DONE				
15.93	200.74	16.5	18.7	52493
23.88	169.36	15.9	15.8	31493
29.16	162.52	7.3	9.1	51197
37.06	95.86	7.4	6.8	31197
44.93	47.03	11.5	10.2	11197
50.15	38.24	11.0	10.5	51182
57.94	13.99	17.3	9.9	31182
65.68	9.64	12.9	16.5	11182
73.37	22.56	8.8	10.4	51121
81.01	41.87	5.7	8.5	31121
88.58	59.28	6.1	6.2	11121
96.09	77.94	5.1	6.0	51140
103.54	82.48	5.6	6.4	31140
110.92	75.16	5.9	5.7	11140
122.63	60.30	5.7	7.0	51158
129.87	46.15	5.7	7.9	31158
137.06	41.26	6.3	7.4	11158

AVERAGE X-SEC 0.0 MB/STR 0 NOTE

INTEGRATED X-SEC 767.11 MB ERROR 7.6 PER CENT

P 7 FIT

L	COEF.	ERROR (O/O)
0	122.08974	2.8
1	16.87875	16.5
2	15.92367	16.1
3	25.27798	8.2
4	12.97415	12.5
5	-1.53077	80.5
6	-1.06600	78.2
7	0.58704	132.5

SCATTERING OF 7.03 +OR-0.06 MEV NEUTRONS FROM O

LEVEL (S) 0.0 MEV KEY (11) 15 ANGLES

ANGLE CM	X-SEC. MB/STR	ERROR (O/O) +	-	RUN

MULTIPLE SCATTERING CORRECTION DONE

29.16	118.61	9.3	7.7	51419
37.06	73.17	10.4	13.4	31419
44.92	49.82	9.1	9.1	11419
50.15	37.65	10.8	7.0	51431
57.94	20.65	15.7	11.0	31431
65.68	16.76	7.3	13.9	11431
73.37	25.63	5.7	10.2	51412
81.00	40.94	5.3	7.0	31412
88.58	59.19	4.7	7.6	11412
96.09	76.67	7.8	7.0	51442
103.54	77.39	4.6	7.9	31442
110.93	73.58	5.6	5.6	11442
122.63	61.98	5.8	5.8	51424
129.87	44.07	5.6	6.5	31424
137.06	36.56	7.0	7.1	11424

AVERAGE X-SEC 0.0 MB/STR 0 NOTE

INTEGRATED X-SEC 745.07 MB ERROR 9.1 PER CENT

P 9 FIT

L	COEF.	ERROR (O/O)
0	118.58188	5.9
1	16.78436	34.3
2	14.09226	42.2
3	20.75504	24.4
4	18.78999	24.0
5	8.64078	41.0
6	3.29581	77.0
7	3.32402	58.5
8	2.02253	58.0
9	1.26456	67.3

SCATTERING OF 7.54 +OR-0.06 MEV NEUTRONS FROM O

LEVEL(S) 0.0 MEV KEY(11) 16 ANGLES

ANGLE CM	X-SEC. MB/STR	ERROR(O/O) +	ERROR(O/O) -	RUN
MULTIPLE SCATTERING CORRECTION DONE				
15.93	238.01	14.2	17.3	51516
29.16	120.42	8.2	8.3	51075
37.06	74.37	9.6	11.3	31075
44.93	47.70	13.3	13.0	11075
50.14	44.72	8.1	11.2	50024
57.94	26.40	12.3	18.1	30024
65.69	25.36	7.4	13.0	10024
73.37	32.69	6.2	11.0	50057
81.01	42.51	6.7	8.4	30057
88.58	59.30	5.3	7.1	10057
96.09	74.42	4.9	7.9	50033
103.53	77.94	5.8	7.0	30033
110.93	74.00	5.8	7.0	10033
122.62	49.91	4.1	8.9	50045
129.87	30.55	5.9	8.3	30045
137.06	18.71	8.6	11.6	10045

AVERAGE X-SEC 0.0 MB/STR 0 NOTE

INTEGRATED X-SEC 723.23 MB ERROR 7.8 PER CENT

P 9 FIT

L	COEF.	ERROR(O/O)
0	115.10646	3.4
1	24.39861	13.3
2	11.30394	26.8
3	23.41467	10.8
4	14.75196	15.0
5	0.52005	364.6
6	3.60260	40.3
7	2.83962	42.3
8	0.71952	115.4
9	0.66956	103.2

SCATTERING OF 8.04 +OR-0.05 MEV NEUTRONS FROM O

LEVEL (S) 0.0 MEV KEY (11) 15 ANGLES

ANGLE CM	X-SEC. MB/STR	ERROR (O/O) +	-	RUN
MULTIPLE SCATTERING CORRECTION DONE				
29.16	105.71	10.4	13.0	51388
37.06	47.42	16.7	14.6	31388
44.93	25.39	17.5	16.8	11388
50.15	23.21	10.4	11.2	51361
57.94	14.60	15.5	16.0	31361
65.68	20.63	13.1	12.3	11361
73.37	35.34	10.1	9.2	51382
81.01	47.61	7.1	11.9	31382
88.58	52.03	7.7	9.6	11382
96.09	55.87	8.7	15.2	51395
103.53	47.56	7.5	8.5	31395
110.93	37.39	7.1	9.0	11395
122.62	28.77	6.6	8.3	51368
129.87	23.58	7.9	7.4	31368
137.06	24.69	9.6	7.4	11368

AVERAGE X-SEC 0.0 MB/STR 0 NOTE

INTEGRATED X-SEC 595.82 MB ERROR 10.4 PER CENT

P 9 FIT

L	COEF.	ERROR (O/O)
0	94.82703	7.6
1	24.63557	25.2
2	17.06117	35.9
3	24.34074	19.7
4	13.71324	31.3
5	0.89908	402.1
6	2.49192	105.4
7	2.51517	83.9
8	1.26619	91.5
9	0.91355	109.2

SCATTERING OF 8.56 +OR-0.05 MEV NEUTRONS FROM O

LEVEL(S) 0.0 MEV KEY(11) 20 ANGLES

MULTIPLE SCATTERING CORRECTION DONE

ANGLE CM	X-SEC. MB/STR	ERROR(O/O) +	ERROR(O/O) -	RUN
15.93	308.35	12.0	12.7	51539
23.88	133.63	19.6	20.2	31539
29.16	91.14	11.6	11.7	51209
37.06	36.38	15.0	12.9	31209
44.92	10.14	28.2	33.4	11209
44.93	10.98	20.4	21.0	51316
50.15	1.45	117.5	57.1	51272
52.75	3.74	95.1	42.5	31316
57.94	7.16	14.3	27.0	32272
60.53	20.31	16.2	10.8	11316
65.68	28.77	9.1	14.5	11272
73.37	50.24	8.2	9.4	51230
81.01	57.74	6.8	11.9	31230
88.58	50.98	12.5	11.6	11230
96.09	57.66	6.7	10.3	51283
103.54	43.84	4.5	8.5	31283
110.92	28.94	11.3	9.5	11283
122.63	25.73	8.8	11.1	51243
129.87	33.84	10.9	7.5	31243
137.06	37.11	9.2	10.6	11243

AVERAGE X-SEC 0.0 MB/STR 0 NOTE

INTEGRATED X-SEC 597.82 MB ERROR 8.2 PER CENT

P 9 FIT

L	COEF.	ERROR(O/O)
0	95.14552	4.3
1	17.11748	18.4
2	14.48577	21.0
3	16.73457	14.0
4	19.31073	10.7
5	10.94458	15.0
6	1.10850	106.8
7	0.71944	152.4
8	0.76742	99.3
9	0.01760	3984.4

SCATTERING OF 7.54 +OR-0.06 MEV NEUTRONS FROM O

LEVEL (S) 6.052 MEV KEY (22) 4 ANGLES
6.131

ANGLE CM	X-SEC. MB/STR	ERROR (O/O) +	-	RUN

MULTIPLE SCATTERING CORRECTION DONE

32.05	39.56	33.1	24.5	51075
40.69	44.22	24.8	24.8	31075
49.24	32.08	29.2	29.4	11075
54.76	25.05	31.4	29.2	50024

AVERAGE X-SEC 34.15 MB/STR O NOTE

INTEGRATED X-SEC 429.08 MB ERROR 27.4 PER CENT

SCATTERING OF 8.04 +OR-0.05 MEV NEUTRONS FROM O

LEVEL (S) 6.052 MEV KEY (22) 5 ANGLES
6.131

ANGLE CM	X-SEC. MB/STR	ERROR (O/O) +	-	RUN

MULTIPLE SCATTERING CORRECTION DONE

53.76	10.43	27.1	21.4	51361
61.85	6.94	24.3	21.5	31361
85.31	8.99	27.0	29.0	31382
93.55	8.96	52.8	25.9	11382
100.97	14.59	23.7	25.6	51395

AVERAGE X-SEC 9.10 MB/STR O NOTE

INTEGRATED X-SEC 114.33 MB ERROR 15.0 PER CENT

SCATTERING OF 8.56 +OR-0.05 MEV NEUTRONS FROM O

LEVEL (S) 6.052 MEV KEY (22) 17 ANGLES
6.131

ANGLE CM	X-SEC. MB/STR	ERROR (O/O) +	-	RUN
MULTIPLE SCATTERING CORRECTION DONE				
30.90	24.91	22.0	20.5	51209
39.28	22.85	14.7	20.4	31209
47.53	18.71	18.3	17.1	11209
47.56	26.15	14.7	11.8	51316
53.00	23.23	11.4	12.2	51272
55.71	25.21	9.9	14.8	31316
61.09	24.26	12.6	13.8	32272
69.12	25.38	37.5	13.8	11272
77.00	22.42	12.3	15.3	51230
84.77	22.22	11.0	17.2	31230
92.44	23.77	10.9	11.2	11230
99.96	25.58	9.2	10.7	51283
107.38	27.64	10.6	10.3	31283
114.65	24.50	9.6	10.0	11283
126.01	28.33	12.5	16.4	51243
132.96	26.72	13.8	13.8	31243
139.84	28.37	16.0	17.9	11243

AVERAGE X-SEC 24.54 MB/STR O NOTE

INTEGRATED X-SEC 308.43 MB ERROR 12.5 PER CENT

ORNL-4780
UC-34 — Physics

INTERNAL DISTRIBUTION

1. Biology Library
2-4. Central Research Library
5. ORNL — Y-12 Technical Library Document Reference Section
6-55. Laboratory Records Department
56. Laboratory Records, ORNL R.C.
57. L. S. Abbott
58. F. S. Alsmiller
59. A. R. Buhl
60. C. E. Clifford
61. F. L. Culler, Jr.
62. J. K. Dickens
63. C. Y. Fu
64. R. F. Hibbs
65. W. H. Jordan
66-75. W. E. Kinney
76. H. G. MacPherson
77-78. F. C. Maienschein
79. C. W. Nestor, Jr.
80. E. M. Oblow
81. S. K. Penny
82-101. F. G. Perey
102. R. W. Roussin
103. M. J. Skinner
104. A. H. Snell
105. D. A. Sundberg
106. A. M. Weinberg
107. R. Q. Wright
108. H. Feshbach (consultant)
109. H. Goldstein (consultant)
110. C. R. Mehl (consultant)
111. H. T. Motz (consultant)

EXTERNAL DISTRIBUTION

112. M. T. McEllistrem, University of Kentucky, Lexington, Kentucky 40506
113. C. E. Hollandsworth, USA Nuclear Effects Lab., Aberdeen Proving Ground, Maryland
114. P. B. Hemmig, Division of Reactor Development and Technology, AEC, Washington, D.C. 20546
115. W. H. Hannum, Division of Reactor Development and Technology, AEC, Washington, D.C. 20546
116. Kermit Laughon, AEC Site Representative, ORNL
117. J. C. Hopkins, Los Alamos Scientific Laboratory, Los Alamos, New Mexico 87544
118. A. B. Smith, Argonne National Laboratory, Argonne, Illinois 60440
119. R. L. Howerton, Lawrence Radiation Laboratory, Livermore, California 94550
120. J. L. Weil, Physics Department, University of Kentucky, Lexington, Kentucky 40506
121. M. D. Goldberg, Brookhaven National Laboratory, Upton, L.I., New York 11973
122. M. Drake, Brookhaven National Laboratory, Upton, L.I., New York 11973
123. P. G. Young, Los Alamos Scientific Laboratory, Los Alamos, New Mexico 87544
124. B. Holmqvist, Studsvik, Nykoping, Sweden
125. C. Le Rigoleur, CEN Cadarache, (13) St. Paul lez Dutrance, France
126. Norman Francis, Knolls Atomic Power Laboratory, General Electric, Schenectady, New York 12309

127. W. E. Tucker, Texas Nuclear Corporation, 5805 Bullard Drive, Austin, Texas 78731
128. Leona Stewart, Los Alamos Scientific Laboratory, Los Alamos, New Mexico 87544
129. J. A. Swartout, Union Carbide Corporation, New York, N.Y. 10017
130. Laboratory and University Division, AEC, ORO
131. Patent Office, AEC, ORO

132-359. Given distribution as shown in TID-4500 under Physics category (25 copies — NTIS)